

Sixth Mississippi State Conference on Differential Equations and Computational Simulations, *Electronic Journal of Differential Equations*, Conference 15 (2007), pp. 163–173. ISSN: 1072-6691. URL: <http://ejde.math.txstate.edu> or <http://ejde.math.unt.edu> <ftp://ejde.math.txstate.edu> (login: ftp)

APPROXIMATIONS OF CONTINUOUS NEWTON'S METHOD: AN EXTENSION OF CAYLEY'S PROBLEM

JON JACOBSEN, OWEN LEWIS, BRADLEY TENNIS

Dedicated to Klaus Schmitt on his 65th birthday

ABSTRACT. Continuous Newton's Method refers to a certain dynamical system whose associated flow generically tends to the roots of a given polynomial. An Euler approximation of this system, with step size $h = 1$, yields the discrete Newton's method algorithm for finding roots. In this note we contrast Euler approximations with several different approximations of the continuous ODE system and, using computer experiments, consider their impact on the associated fractal basin boundaries of the roots.

1. INTRODUCTION

In many contexts and applications one is faced with the task of finding a value x such that $f(x) = 0$ for a given function f . Despite being a relatively easy problem to state, for certain choices of f , this task may be formidable. In the late 17th century Newton considered an iterative method to find zeros of real-valued functions $f : \mathbb{R} \rightarrow \mathbb{R}$. Starting with an initial seed value x_0 , Newton proposed the iterative method

$$x_{n+1} = x_n - \frac{f(x_n)}{f'(x_n)} \quad x_n \in \mathbb{R}, \quad (1.1)$$

to generate a sequence $\{x_n\}$ that converges to a root of f . In 1870 Schröder [11] and in 1879, Cayley [2] imitated the method for complex polynomials $p(z)$ and considered the behavior of sequences

$$z_{n+1} = z_n - \frac{p(z_n)}{p'(z_n)} \quad z_n \in \mathbb{C}. \quad (1.2)$$

For quadratic polynomials Cayley found that the method did indeed converge to a root. Moreover, he proved (via conjugation to the map $z^2 + c$) that the complex plane could be divided into two half-planes, such that seeds in either half converged to the unique root lying in its own half. In other words, Cayley characterized the global basins of attraction $A(\xi) = \{z_0 \in \mathbb{C} : z_n \rightarrow \xi\}$ for each root ξ .

Having succeeded in the quadratic case, Cayley remarked that “the next succeeding case of the cubic equation appears to present considerable difficulty.” The

2000 *Mathematics Subject Classification*. 34C35, 58C15, 28A80, 65H10.

Key words and phrases. Newton's method; damping; fractal basins of attraction.

©2007 Texas State University - San Marcos.

Published February 28, 2007.

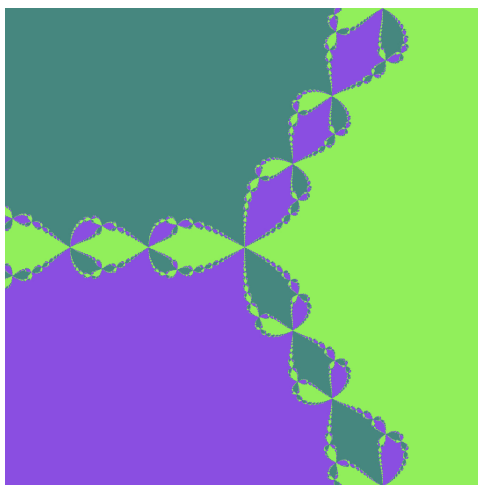


FIGURE 1. Basins of Attraction for $p(z) = z^3 - 1$.

task of identifying such basins for complex polynomials is now known as *Cayley's Problem*. Nearly 40 years later, work of French mathematicians Julia and Fatou [6, 4] shed much light on Cayley's difficulties in their groundbreaking study of iterating complex rational mappings. In particular, for polynomials, the right-hand side of (1.2) represents a rational map of the extended complex plane to itself and their work implies that the basins of the three roots share a common boundary, the so-called *Julia set* of $p(z)$. Without having seen an example before, it is hard to imagine a ternary division of the complex plane such that every point on the boundary of one set is also on the boundary of the other two sets. In other words, imagine partitioning the plane into three "states" such that every point on the border of one state also simultaneously lies on the border of the other two states. Basins of attraction with this property are said to satisfy the Wada property, a concept introduced by Japanese mathematician Konizō Yoneyama [14] in 1917.

In the early 1980's, and just over a century after Cayley's work, computer simulations allowed one to visualize Cayley's basins and their associated fractal structure. For the cubic $p(z) = z^3 - 1$ the basins are captured by the image in Figure 1. Although a familiar image now, it is hard to imagine to what degree Cayley, Julia, Fatou and other early researchers imagined these basins to look like.

In hindsight, one can understand why Schröder and Cayley's approach worked. We now recognize that the Newton map (1.2) is precisely an Euler approximation of the differential equation

$$z'(t) = -\frac{p(z(t))}{p'(z(t))}, \quad t > 0, \quad (1.3)$$

with step size $h = 1$. Equation (1.3) is known as *Continuous Newton's Method*. If $z(t)$ solves (1.3) with $z'(t) \rightarrow 0$ as $t \rightarrow \infty$, then it should be that $z(t)$ converges to a root of p . Indeed, suppose $z(t)$ solves (1.3) with $z(0) = z_0$. Assuming $p(z(t)) \neq 0$ for $t > 0$, then it follows $\frac{p'(z)}{p(z)} \dot{z}(t) = -1$, or equivalently, $p(z(t)) = p(z_0)e^{-t}$. Thus, solutions $z(t)$ flow to a zero of p while keeping the argument of $p(z(t))$ constant at

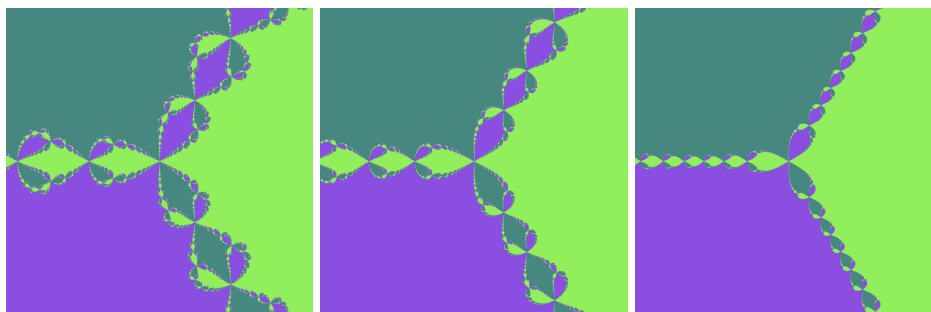


FIGURE 2. Basins for $p(z) = z^3 - 1$ with damped Newton method:
 $h = 1.3, 0.9, 0.4$ respectively.

$\arg(p(z_0))$. In this way we can view Newton's method (for real or complex polynomials) as an approximation to this flow, which leads to roots in most cases. For example, if $p(z) = z^3 - 1$, then we can explicitly solve for $z(t) = \sqrt[3]{(z_0^3 - 1)e^{-t} + 1}$, where the appropriate branch of the cube root is chosen corresponding to the nearest root of $p(z)$. In this case, the corresponding basins of attraction are defined by the ternary division of the plane defined by the rays $\theta = \frac{\pi}{3}, \theta = -\frac{\pi}{3}$, and $\theta = \pi$, as suggested by the rightmost image in Figure 2. This is the cubic analog of the binary division Cayley found for quadratic polynomials.

From this point of view, the fractal basin boundaries that arise in Newton's method (such as those in Figures 1 and 2) are due to the discretization of the Continuous Newton flow (1.3). In one sense, the complex boundaries arise from the numerical error inherent in the approximation of the flow.

The first author to recognize the relevance of the continuous Newton method to classical Newton's method appears to be Smale [12], in his work on finding equilibrium points. Several other authors, including Hirsch and Smale [5], Braess [1], Saupe [10], Peitgen, Prüfer, and Schmitt [9], and Neuberger [8], have also considered aspects of continuous methods. In particular, the continuous Newton's method (1.3) leads one to consider the damped Newton algorithm defined by approximating (1.3) using Euler's method with step size h :

$$x_{n+1} = x_n - h \frac{f(x_n)}{f'(x_n)}, \quad x_n \in \mathbb{R}, \quad (1.4)$$

for $0 < h < 2$ (when $h = 2$ the fixed points of (1.4) become repelling). Neuberger [8] observed that the associated Cayley basins get larger and their fractal boundary structure shrinks away as $h \rightarrow 0$, as indicated in Figure 2. This is in agreement with the fact that smaller step sizes lead to improved accuracy in the approximation of equation (1.3).

With this in mind, in this paper we consider how the fractal boundaries behave with respect to improved numerical integration techniques. For instance, what do the basins look like if one uses a Runge-Kutta algorithm on (1.3) instead of the Euler method? How do the sizes of the fractal basin boundaries compare for different step sizes and different methods? Methods such as Runge-Kutta provide higher-order accuracy, but their associated iterative map (for a given step size) is also more complex (e.g., than (1.4)). With this in mind, we consider several numerical

schemes for approximating (1.3) and compare their associated Cayley basins. We consider this in the context of complex polynomials as well as for general vector fields on \mathbb{R}^n . For related work based on altering explicitly the discrete iterative step (1.4) see Varona [13] and Epureanu et al. [3].

2. REFINED ALGORITHMS

In this section we consider six different numerical algorithms for approximating Continuous Newton's Method (1.3). For each method we consider the associated fractal basin boundaries for the cubic $p(z) = z^3 - 1$, for a range of step sizes. We first define the methods in the context of solving $\frac{dy}{dt} = f(t, y)$, using w_i for the iterations and h for the step size. The six methods we consider are:

- Euler's Method. This basic numerical technique with step size h leads to the iterative scheme known as Damped Newton's Method:

$$w_{i+1} = w_i + h f(t_i, w_i).$$

- Refined Euler. The refined Euler's method performs a size $\frac{h}{2}$ Euler step and uses this result to perform midpoint integration:

$$w^* = w_i + \frac{h}{2} f(t_i, w_i)$$

$$w_{i+1} = w_i + h f\left(t_i + \frac{h}{2}, w^*\right).$$

- Heun's Method. Another refined Euler method, this method performs a size h Euler step and uses this result to perform trapezoidal integration:

$$w^* = w_i + h f(t_i, w_i)$$

$$w_{i+1} = w_i + \frac{h}{2} [f(t_i, w_i) + f(t_i + h, w^*)].$$

- Runge-Kutta (Order 2). Though the Refined Euler method and Heun's method are also second order Runge-Kutta methods, this method is an optimal one in the sense that its coefficients are chosen to minimize the error in the approximation of the Taylor series of y :

$$w^* = w_i + \frac{2h}{3} f(t_i, w_i)$$

$$w_{i+1} = w_i + \frac{h}{4} [f(t_i, w_i) + 3f(t_i + \frac{2h}{3}, w^*)].$$

- Runge-Kutta (Order 4). The classical fourth order Runge-Kutta method is defined by:

$$k_1 = h f(t_i, w_i)$$

$$k_2 = h f\left(t_i + \frac{h}{2}, w_i + \frac{k_1}{2}\right)$$

$$k_3 = h f\left(t_i + \frac{h}{2}, w_i + \frac{k_2}{2}\right)$$

$$k_4 = h f(t_i + h, w_i + k_3)$$

$$w_{i+1} = w_i + \frac{1}{6}(k_1 + 2k_2 + 2k_3 + k_4).$$

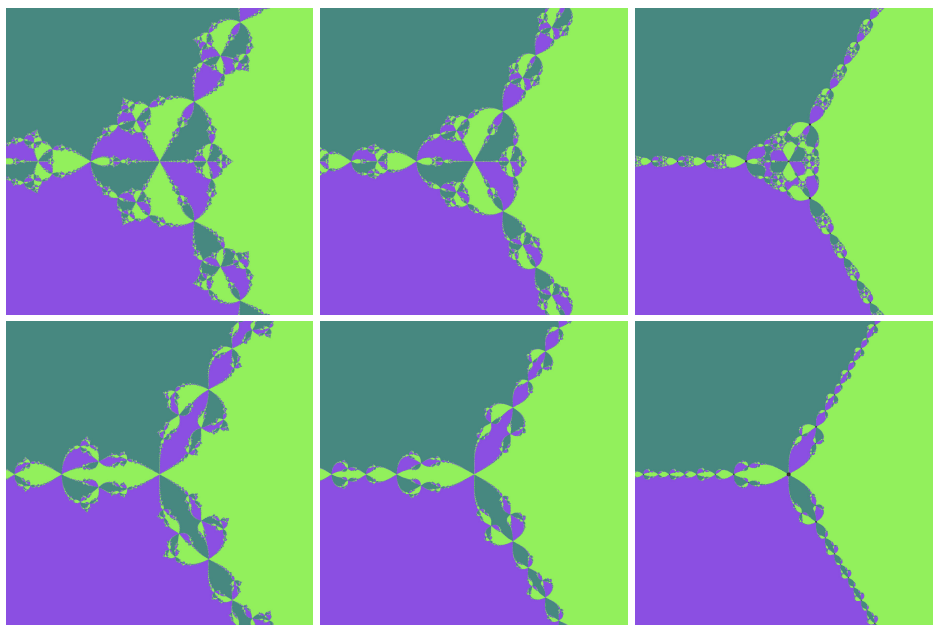


FIGURE 3. Basins for $p(z) = z^3 - 1$ with (top): Refined Newton method; (bottom): Heun's method. The images reflect step sizes (from left to right) of $h = 1.4, 0.9$, and 0.4 .

- Adams-Bashforth (Order 2). The two-step Adams-Bashforth method is a second order multi-step method. The initial iterate is assigned to w_0 and w_1 is calculated using a second order Runge-Kutta approximation:

$$\begin{aligned}
 w^* &= w_0 + \frac{2h}{3}f(t_i, w_0) \\
 w_1 &= w_i + \frac{h}{4}\left[f(t_i, w_0) + 3f\left(t_i + \frac{2h}{3}, w^*\right)\right] \\
 w_{i+1} &= w_i + h\left[\frac{3}{2}f(t_i, w_i) - \frac{1}{2}f(t_{i-1}, w_{i-1})\right].
 \end{aligned}$$

For each method we apply the associated iterative map for each point in the region $[-1.5, 1.5] \times [-1.5, 1.5] \subset \mathbb{R}^2$, using a mesh of 1024×1024 . Each point is iterated and colored according to which root the orbit converges to. We use a tolerance of $\epsilon = 1 \times 10^{-10}$ for determining which root, and set the maximum iterations at 500. Figures 3 and 4 contain select computed basins for three fixed step sizes: $h = 1.4, 0.9$, and 0.4 . The corresponding images for Newton's method appear in Figure 2. In addition to considering the basins for fixed step size h , one can also consider the dynamic flow of the basins as the step size is continuously varied. The accompanying website [7] contains several such movies.

Due to the Wada property, any neighborhood of a point on a basin boundary will contain points whose associated iteration will converge to each and every root of the polynomial. In particular, trajectories corresponding to arbitrarily close initial data on the boundary will have divergent orbits. In this sense the boundary describes the unstable set for a given approximation. In order to compare the

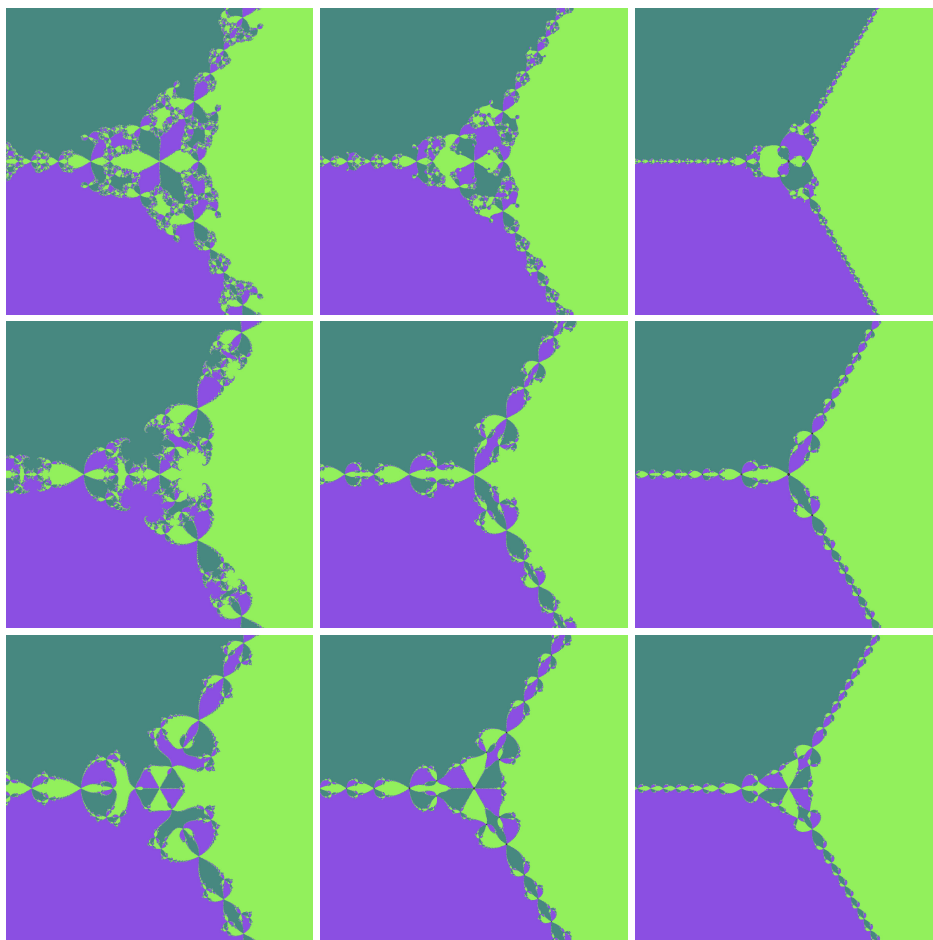


FIGURE 4. Basins for $p(z) = z^3 - 1$ with (top): Runge-Kutta, Order 4 method; (middle): Runge-Kutta, Order 2 method; (bottom): Adams-Bashforth, Order 2 method. The images reflect step sizes (from left to right) of $h = 1.4, 0.9,$ and 0.4 .

complexity of these unstable sets we estimate their fractal dimension using a box-counting algorithm. With this approach we find several interesting dynamics with respect to the variation in fractal dimension. In particular, better algorithms did not necessarily produce basin boundaries with smaller fractal dimension. Several sample dimension comparisons are shown in Figure 5.

Although in many cases the higher-order approximations lead to basins with smaller fractal dimension, the associated computation time can also be significantly larger, given the higher complexity of the algorithm.

3. NEWTON'S METHOD IN \mathbb{R}^n

There is a natural extension of continuous Newton's method to higher dimensional systems. Namely, for $G : \mathbb{R}^n \rightarrow \mathbb{R}^n$ the associated continuous flow for

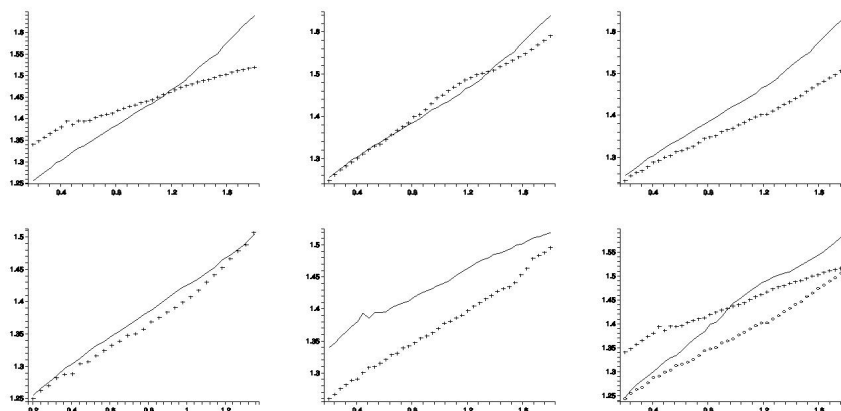


FIGURE 5. Fractal dimension vs. step size for (a) Euler (line) vs. Refined Euler (cross); (b) Euler (line) vs. Runge-Kutta Order 4 (cross); (c) Euler (line) vs. Heun (cross); (d) Euler (line) vs. Runge-Kutta Order 2 (cross); (e) Refined Euler (line) vs. Adams-Bashforth (cross); (f) Runge-Kutta Order 4 (line), Refined Euler (cross), Heun (diamond).

$x : \mathbb{R} \rightarrow \mathbb{R}^n$ is

$$\dot{x} = -[DG(x(t))]^{-1}G(x(t)), \quad (3.1)$$

where DG is the Jacobian matrix of the vector field G . The flow is defined for $x \notin \mathcal{S}$, where

$$\mathcal{S} = \{x \in \mathbb{R}^n : \det DG(x) = 0\}, \quad (3.2)$$

is the singular set of G . The Euler approximation of (3.1) with step size $h = 1$ yields Newton's Method for \mathbb{R}^n :

$$x_{n+1} = x_n - [DG(x_n)]^{-1}G(x_n). \quad (3.3)$$

In this case, we have left the realm of rational maps of the complex plane, and the theory of iterated rational maps no longer applies. For example, the basin boundaries need not be common and there is no known general characterization as precise as the Julia and Fatou set theory for complex maps. Peitgen, Prüfer, and Schmitt [9] suggest the following candidates for the Julia-like sets for discretizations of (3.1):

$$\mathcal{J}_h = \{x \in \mathbb{R}^n : N^k(z) \in \mathcal{S} \text{ for some } k \in N\}, \quad (3.4)$$

where N is an associated iterative map based on a discretization of (3.1) with step size h , and N^k denotes the k^{th} iteration of N . To illustrate the dynamics of the generalized continuous Newton's Method we follow Peitgen et al. [9] and consider vector fields G that arise from discretizing the nonlinear boundary value problem

$$\begin{aligned} u'' + \lambda(u - u^2) &= 0, & 0 < x < 1, \\ u(0) &= u(1) = 0. \end{aligned} \quad (3.5)$$

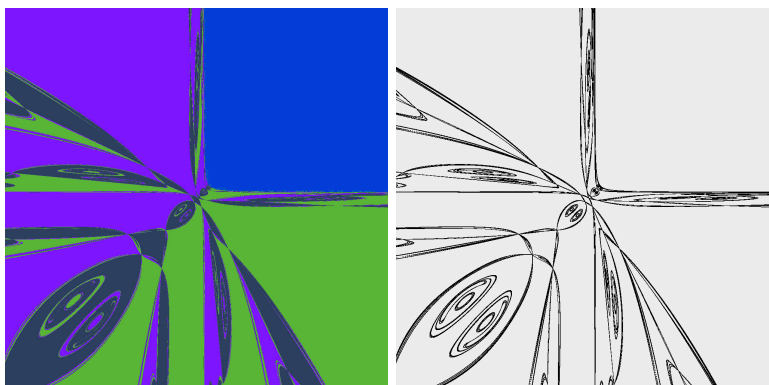


FIGURE 6. Basins of attraction (left) and singular set (right) for (3.6) with Euler approximations for $\mu = 3.2$ and $h = 1.6$. This singular set example is due to Peitgen et al. [9].

A centered difference approximation with a two point interior mesh for the system (3.5) yields the vector field $G : \mathbb{R}^2 \rightarrow \mathbb{R}^2$ defined by

$$G(x, y) = \begin{bmatrix} 2x - y - \mu(x - x^2) \\ 2y - x - \mu(y - y^2) \end{bmatrix}, \quad (3.6)$$

where $\mu = -\frac{\lambda}{9}$. That is, roots of G yield approximate values of solutions to (3.5) at the two interior mesh points. To illustrate the dynamics, we consider the system for $\mu = 3.2$, for which (3.5) has four solutions given by the trivial solution, the positive solution, and two sign-changing solutions (one the negative of the other). Figure 6 shows a comparison of the basin boundaries of the four roots with the singular set, showing a good match. Notice that in this setting the basin boundaries do not satisfy the Wada property. In particular, the basin for the positive solution does not meet the other basins, other than on the border in the first quadrant.

In Figure 7 we show the corresponding images for three additional methods. In each of these examples the associated singular set defined by (3.4) corresponded with the basin boundaries. Again, the boundary for the positive root does not meet the other basins, other than in a small neighborhood of the first quadrant.

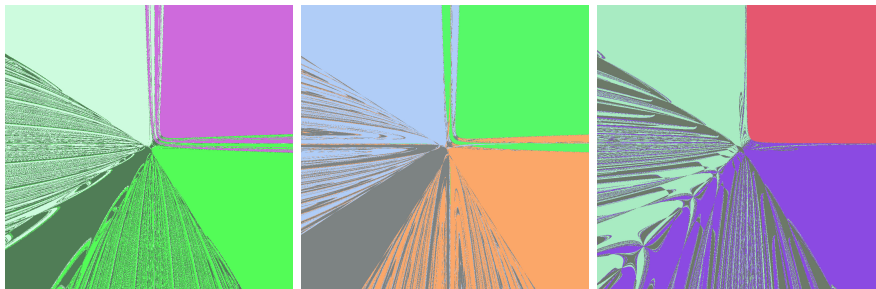


FIGURE 7. Basins of attraction for (3.6) with $\mu = 3.2$, and $h = 1.6$ using (left) Runge-Kutta Order 4; (middle) Adams-Bashforth; and (right) Heun's Method.



FIGURE 8. Basins of attraction (left) and singular set (right) for (3.6) with Euler approximations (similar images result for the other methods) with $\mu = 2.1$, and $h = 1.2$. With only two roots, the basin boundaries do not capture the singular set.

Generically, the basins of attraction alone need not reveal the singular set. For example, Figure 8 shows a comparison of the basins with the singular set for $\mu = 2.1$. In this case (3.5) has only the trivial solution and the positive solution, and the basins do not reflect the singular set. This is true generically for the case $1 < \mu < 3$, for which equation (3.5) has only the the trivial and positive solution (compare to Figure 6, with three nonpositive solutions). Further properties of the orbits can reveal the singular set. For example, Peitgen et al. demonstrate that the singular set structure can be revealed by further partitioning the basins into level sets based on rates of convergence [9].

The images in this article were generated using C++ code. We have developed an application that allows the interested reader to generate their own images, or sequence of images, for any two dimensional vector field of interest [7]. This reference also contains several movies that accompany the material in this paper, and give further insight into the global dynamics for these different methods. In particular, the movies show very clearly how the basins vary as the step size h varies. For each system, when h is sufficiently small, the images appear the same, up to a small rescaling, such as demonstrated in Figure 2. However, this is not generically true. For example, the approximation methods in Figure 4 show notable differences in the basins for the same three step size parameters used in Figure 2.

Finally, it is interesting to note the behavior of the basins as h approaches the critical value for which the roots become repelling fixed points. To illustrate the complexity that can arise we end with a few images near the edge of stability in Figure 9.

Acknowledgments. We would like to thank John M. Neuberger (Northern Arizona University) for many helpful discussions on the ideas in this paper.

REFERENCES

- [1] D. Braess, *Über die Einzugsbereiche der Nullstellen von Polynomen beim Newton-Verfahren*, Numer. Math. **29** (1977/78), no. 1, 123–132.

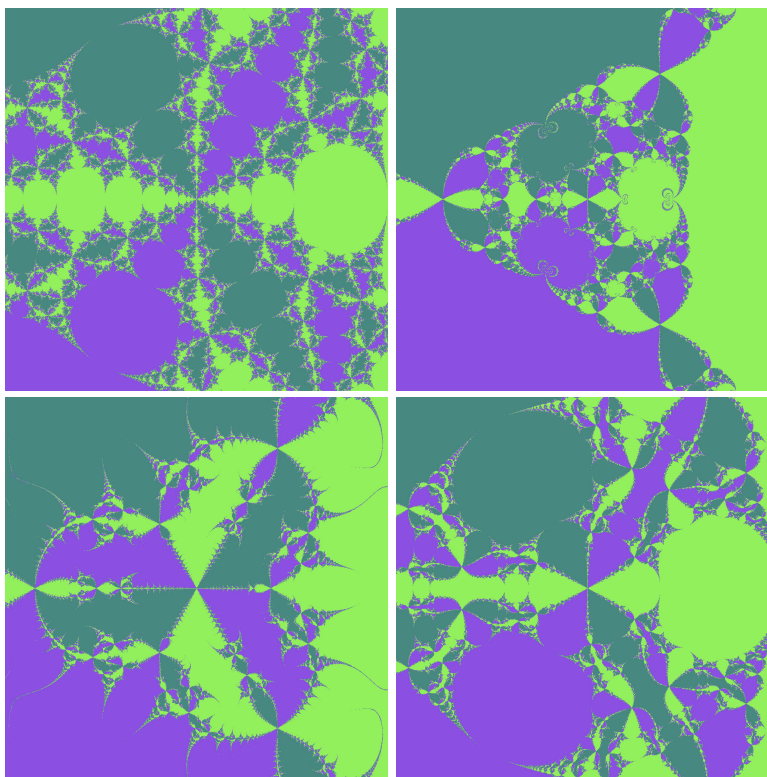


FIGURE 9. Basins on the edge of stability for: (top left) Newton's Method, $h = 1.995$; (top right) Runge-Kutta Order 2, $h = 1.354$; (bottom left) Adams-Bashforth, $h = 1.999$; (bottom right) Heun's method, $h = 1.995$. Reference [7] contains several animations of the basins as the step size is varied from the stable to the unstable regime.

- [2] A. Cayley, *Desiderata and suggestions. No. 3.-the Newton-Fourier imaginary problem*, Amer. J. Math **2** (1879), no. 1, 97.
- [3] B. I. Epureanu and H. S. Greenside, *Fractal basins of attraction associated with a damped Newton's method*, SIAM Rev. **40** (1998), no. 1, 102–109 (electronic).
- [4] P. Fatou, *Sur les equations fonctionnelles*, Bull. Soc. Math., France **47–48** (1919–1920), 161–314.
- [5] M. W. Hirsch and S. Smale, *On algorithms for solving $f(x) = 0$* , Comm. Pure Appl. Math. **32** (1979), no. 3, 281–313.
- [6] G. Julia, *Memoire sur l'iteration des fonction rationnelles*, J. Math. Pures et Appl. **81** (1918), 47–235.
- [7] Magifrac, *Available electronically*, <http://www.math.hmc.edu/magifrac/>.
- [8] J. W. Neuberger, *Continuous Newton's method for polynomials*, Math. Intelligencer **21** (1999), no. 3, 18–23.
- [9] H.-O. Peitgen, M. Prüfer, and K. Schmitt, *Global aspects of the continuous and discrete Newton method: a case study*, Acta Appl. Math. **13** (1988), no. 1-2, 123–202.
- [10] D. Saupe, *Discrete versus continuous Newton's method: a case study*, Acta Appl. Math. **13** (1988), no. 1-2, 59–80.
- [11] E. Schröder, *Ueber unendlich viele algorithmen zur auflösung der gleichungen*, Math. Ann. **2** (1870), 317–365.

- [12] S. Smale, *A convergent process of price adjustment and global Newton methods*, J. Math. Econom. **3** (1976), no. 2, 107–120.
- [13] J. L. Varona, *Graphic and numerical comparison between iterative methods*, Math. Intelligencer **24** (2002), no. 1, 37–46.
- [14] K. Yoneyama, *Theory of continuous sets of points*, Tohoku Math. J. **12** (1917), 43–158.

JON JACOBSEN

MATHEMATICS DEPARTMENT, HARVEY MUDD COLLEGE, 301 PLATT BLVD, CLAREMONT, CA 91711,
USA

E-mail address: `jacobsen@math.hmc.edu`

OWEN LEWIS

4047 NORTH CASTLE AVE., PORTLAND, OR 97227, USA

E-mail address: `owen.lewis@gmail.com`

BRADLEY TENNIS

COMPUTER SCIENCE DEPARTMENT, STANFORD UNIVERSITY, STANFORD, CA 94305, USA

E-mail address: `btennis@stanford.edu`